3rd World Congress on Petrochemistry and Chemical Engineering
Nov. 30 – Dec. 02, 2015
Atlanta, GA

A Robust Image Analysis Approach for High Void-Fraction Gas-Liquid Flows

Ashish Karn, Roger E A Arndt, Jiarong Hong

Department of Mechanical Engineering &
Saint Anthony Falls Laboratory
University of Minnesota Twin Cities, Minneapolis, MN

St. Anthony Falls Laboratory
University of Minnesota

U.S. DEPARTMENT OF ENERGY

DEPARTMENT OF THE NAVY ONR Science & Technology

Bubbly flows occur frequently in natural systems.

Bubbly Flows

Used in petroleum, energy-producing and chemical industries.

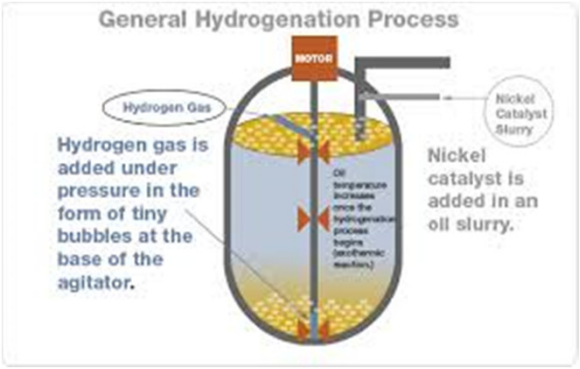

Bubble Columns

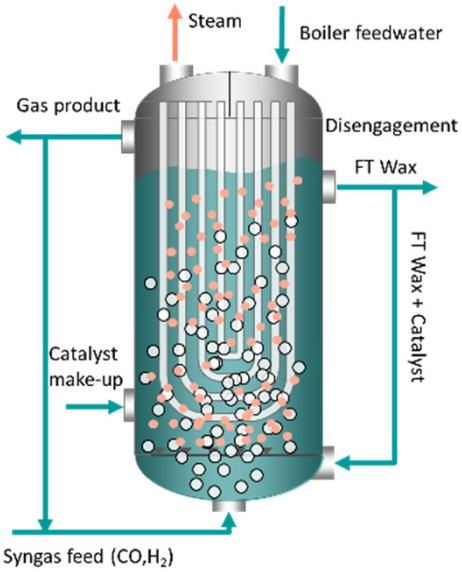

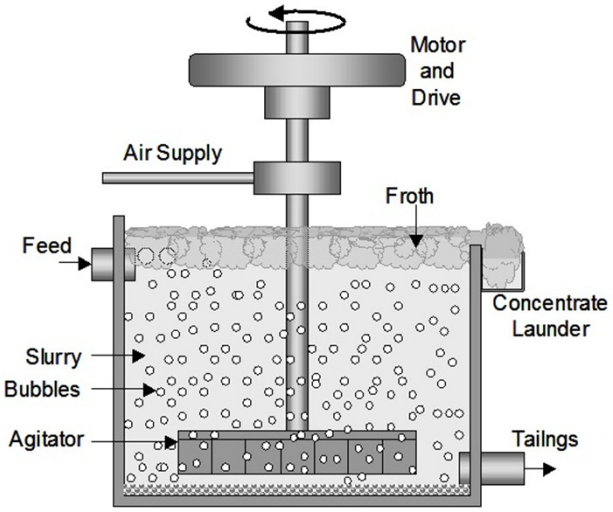

Floatation cells

Measuring Bubble Size Distribution

- Employed in a variety of chemical/biochemical processes:
  - Fischer-Tropsch process for hydrocarbon synthesis
  - Hydrogenation of unsaturated oil
  - Coal liquefaction
  - Fermentation
  - Wastewater treatment

- The concentration distribution and morphology of the bubbles affects:
  - Interfacial area available for chemical reactions,
  - Pressure drop,
  - Heat and mass transfer

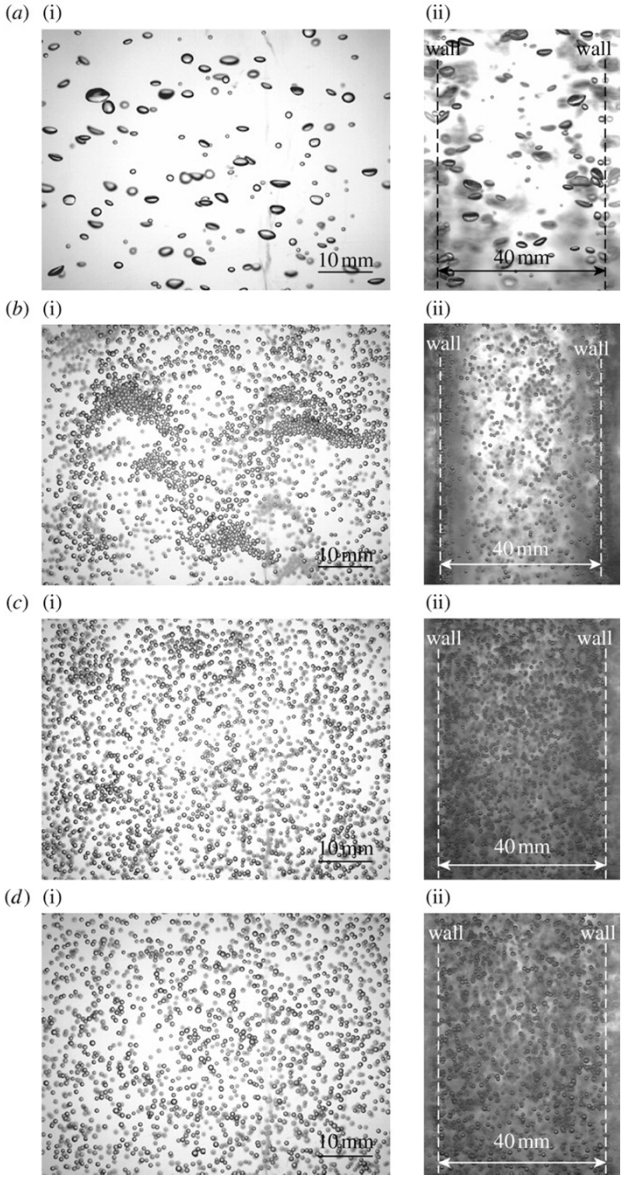

Measurement Techniques

Intrusive

- Capillary suction probes
- Conductivity Probes
- Optical Fiber Probes
- Wire-mesh sensors

Non-intrusive

- Interferometric Particle Imaging
- Laser Doppler Velocimetry
- Phase Doppler Velocimetry
- **Digital Image Analysis**

Digital Image Analysis

Advantages

- Flexibility
- Insensitivity to the optical properties of the dispersed phase
- Easier optics alignment
- Simultaneous information on velocity and size of the dispersed phase

Challenges

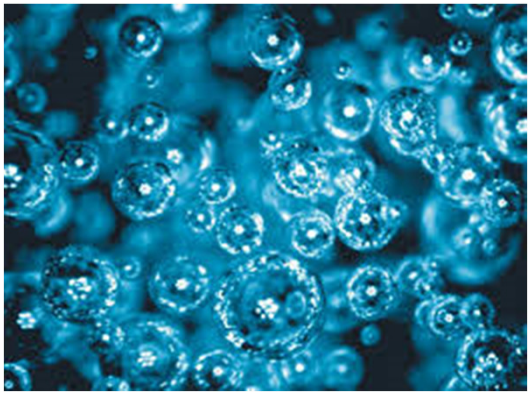

- Computational Speed for real-time image processing
- Ability to cope up with the poor quality of images
- Robustness – capability to resolve overlapped clusters

Relevance of the current research

Develop aeration technology for hydroturbines to minimize environmental impact.

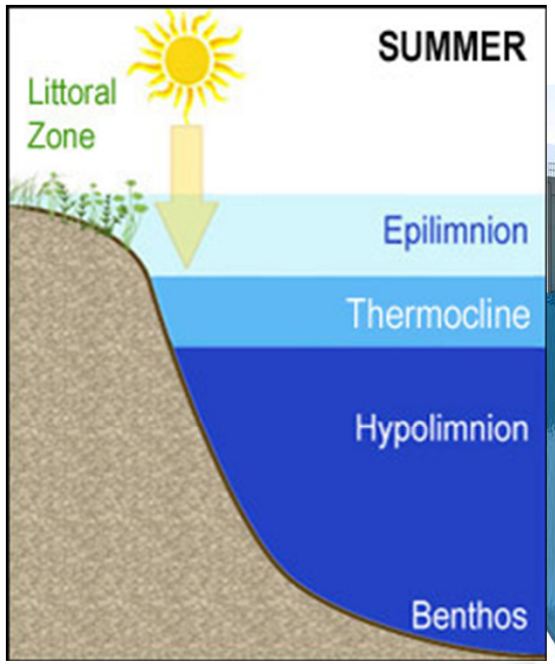

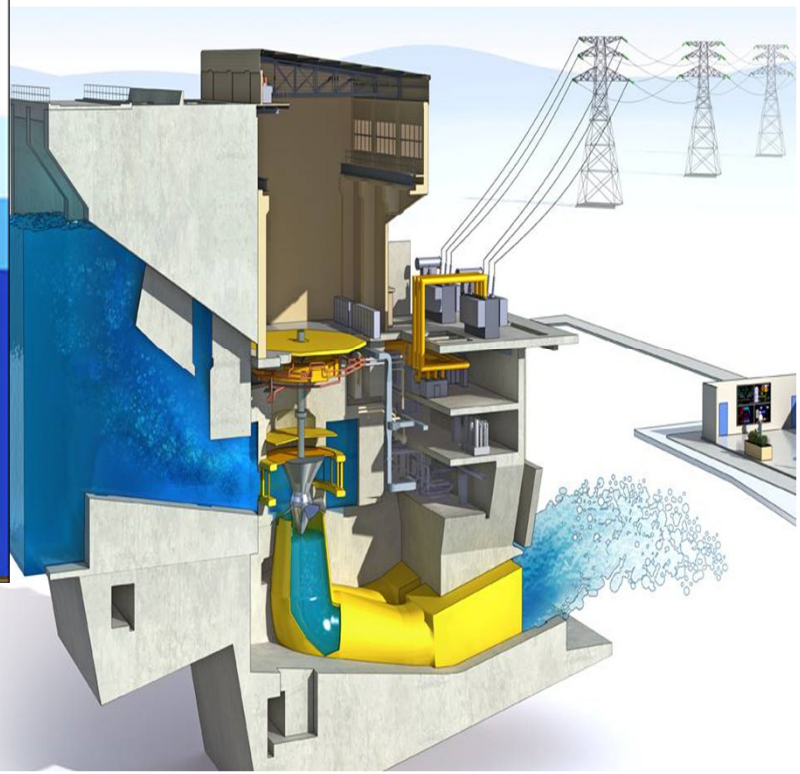

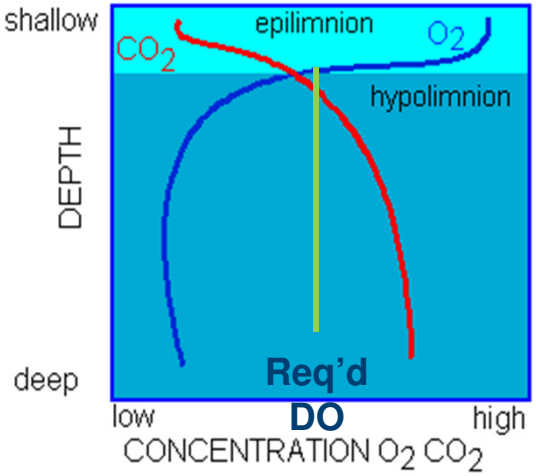

Experimental Facility

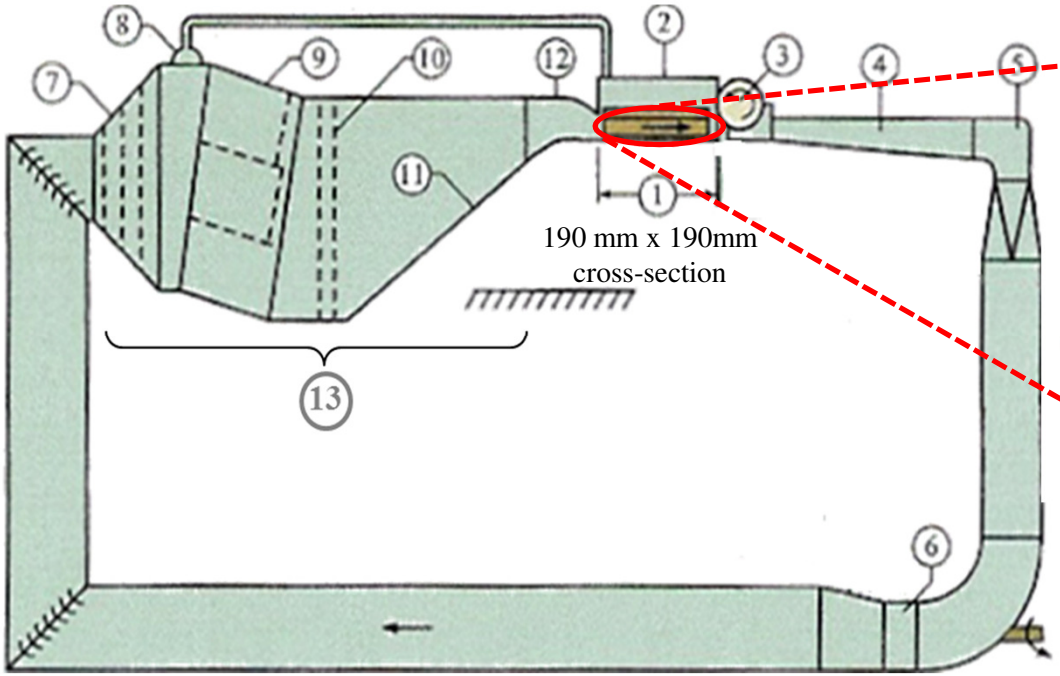

SAFL High Speed Water Tunnel

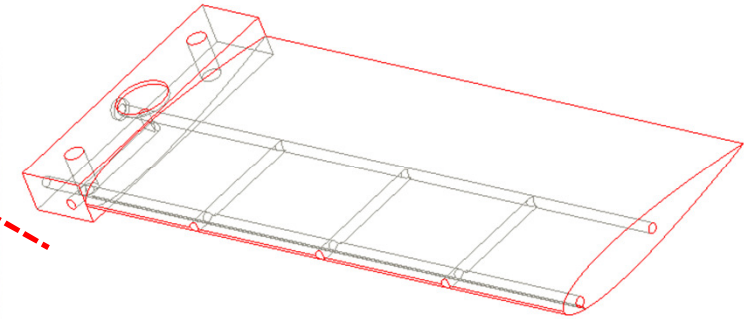

Ventilated hydrofoil
(Turbine blade)

A vented turbine blade was mounted in a High speed water tunnel, and bubble data was recorded in its wake.

Experimental Methodology

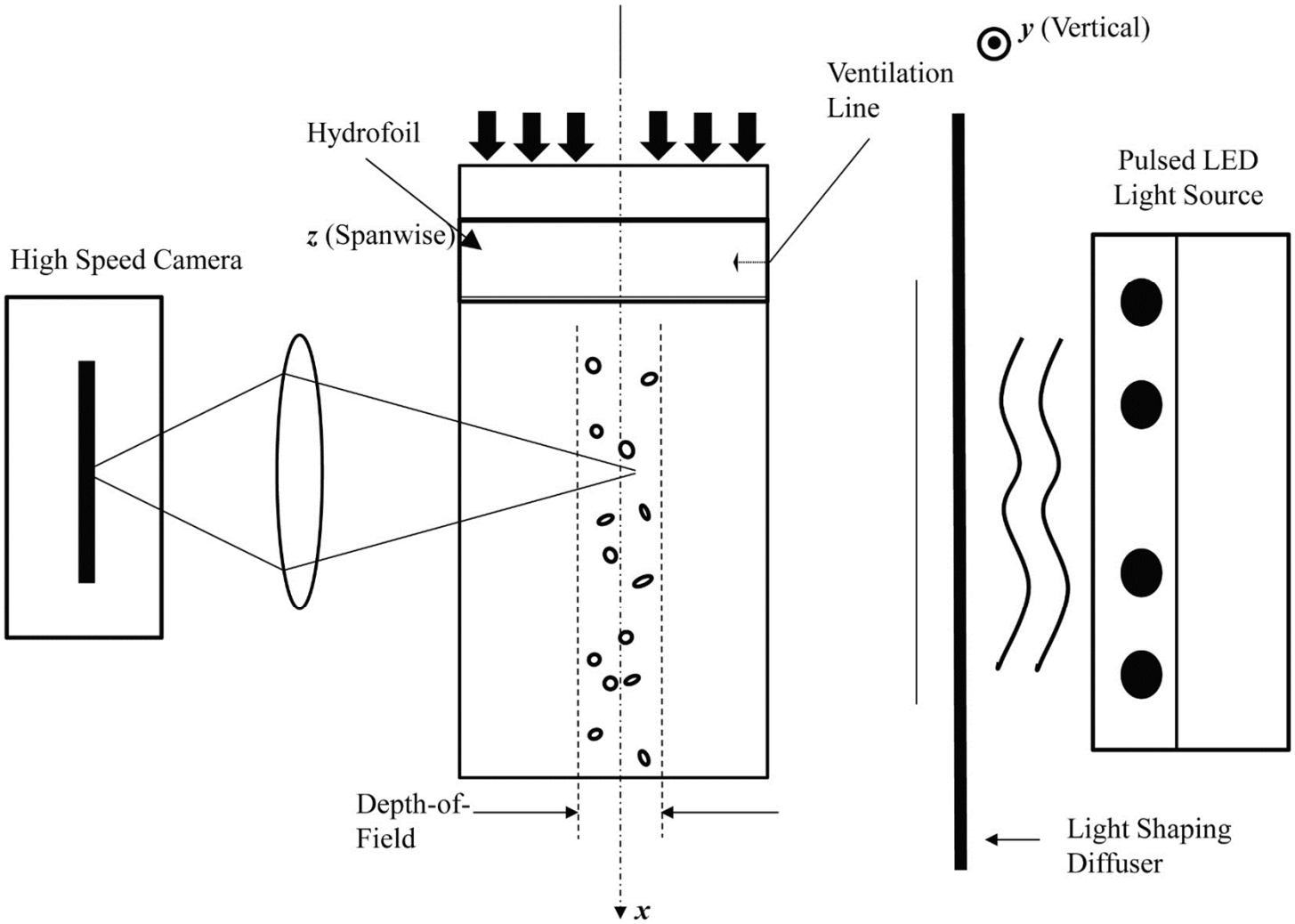

Shadow Image Velocimetry Set up (Karn et al. *Chem. Eng. Sci.* 2015*a*)

Experiments and Data Acquisition

1. Test section, 1.20m x 0.19m x 0.19m
2. Test section dome
3. Skimmer
4. 7° diffuser
5. Guide vane elbow
6. Axial flow pump, 150 HP
7. Diffuser screens
8. Gas collector dome
9. Gas separator, 2134D
10. Honeycomb
11. Contraction
12. Nozzle
13. Settling Chamber

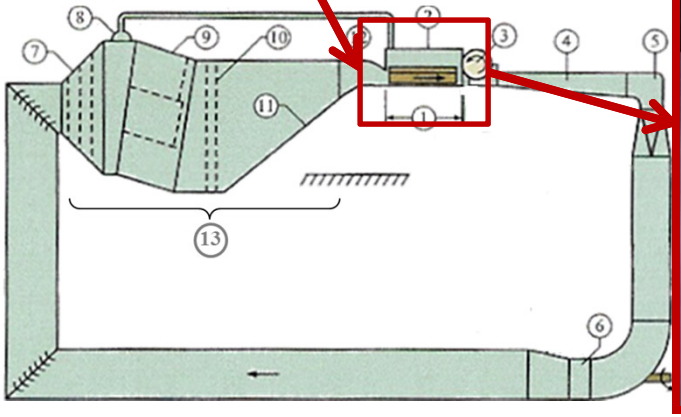

Schematic of SAFL water tunnel

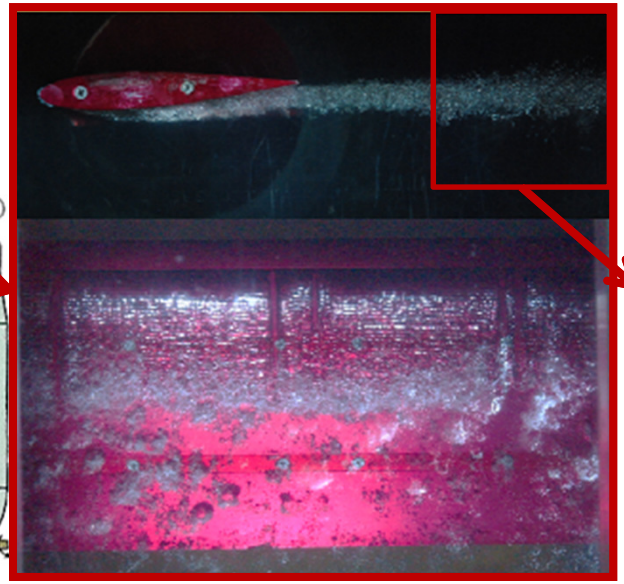

Testing with leading edge aeration

Sample Bubble image

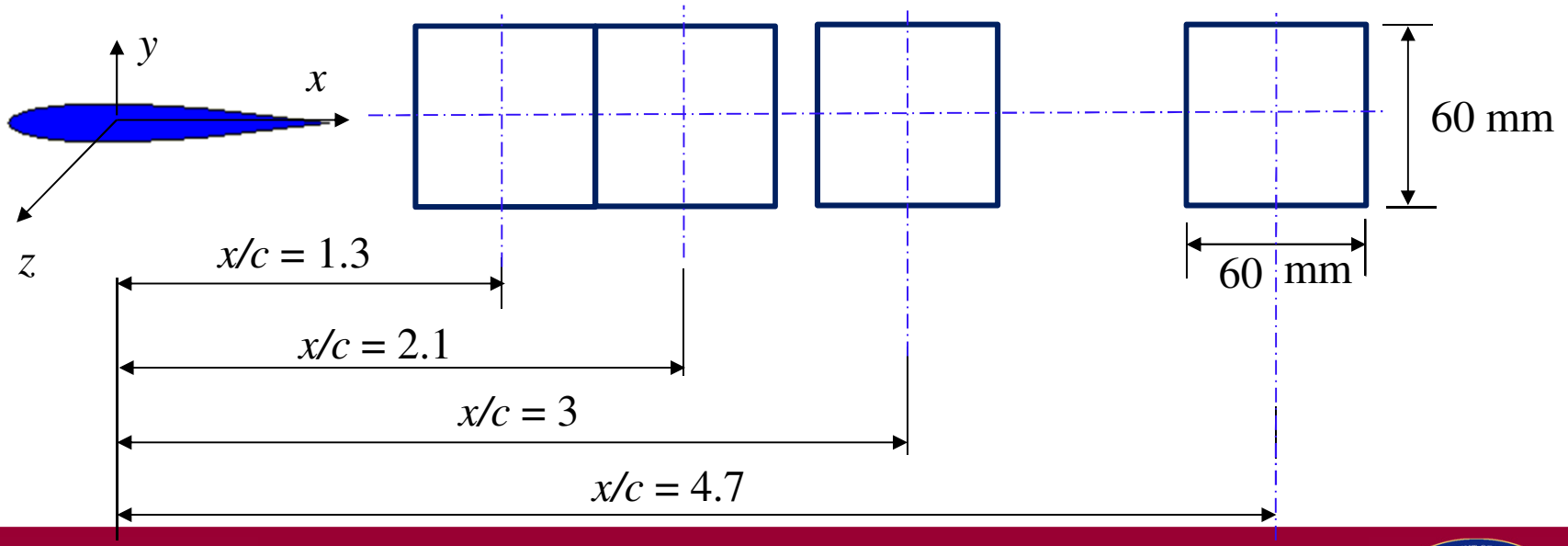

Image Analysis Technique

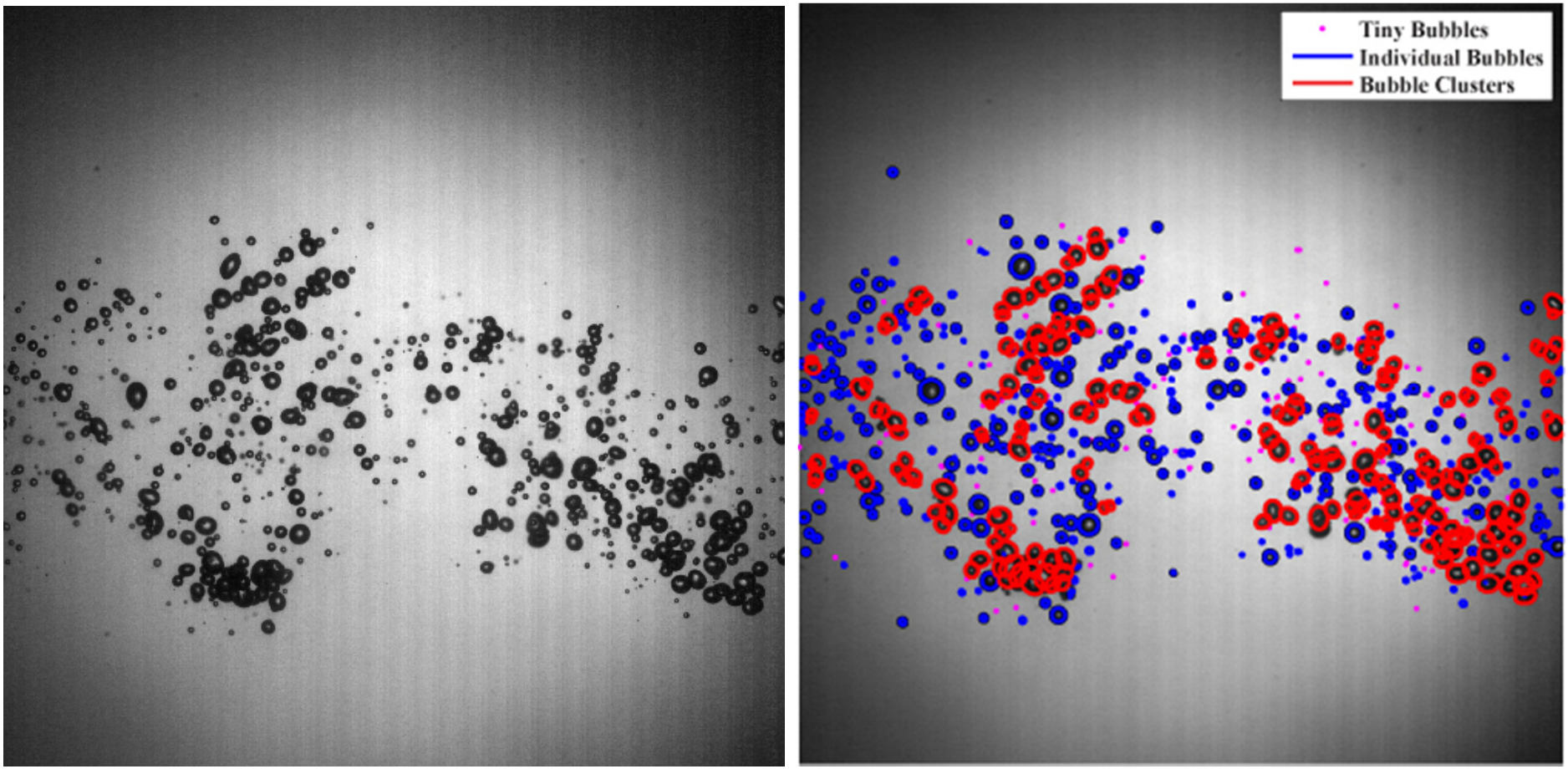

- Image analysis technique resolves bubbles from clusters.
- Size and shape information of both in-focus/out-of-focus bubbles are obtained.

Image Analysis Technique

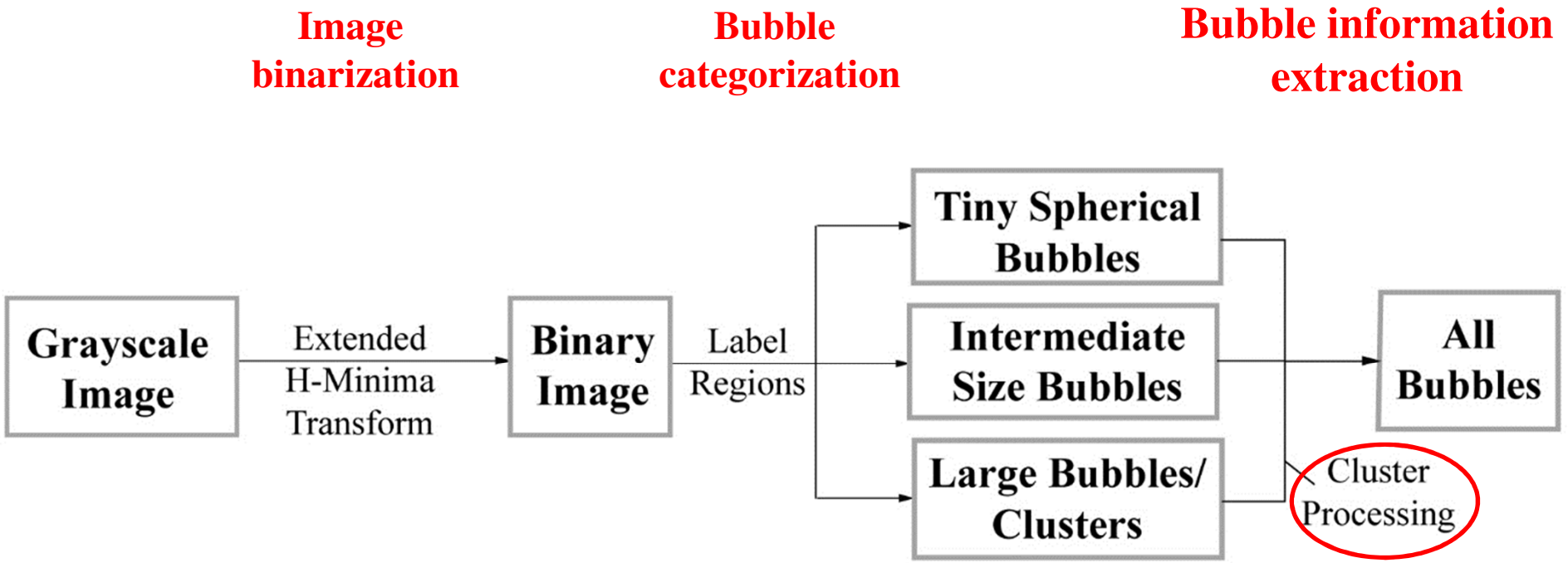

Overview of the Image analysis technique

Cluster Processing

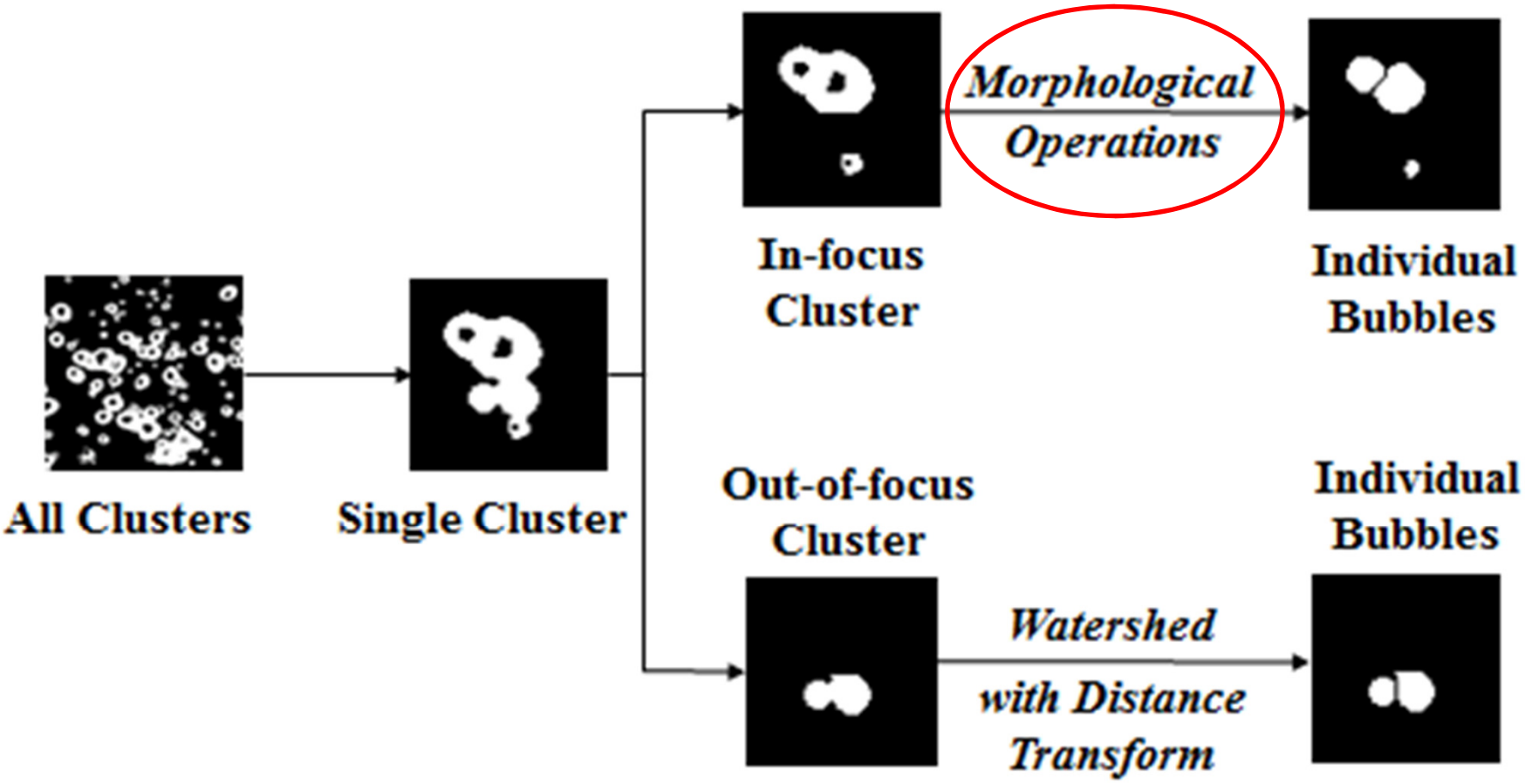

Morphological operations : In-focus Cluster Processing

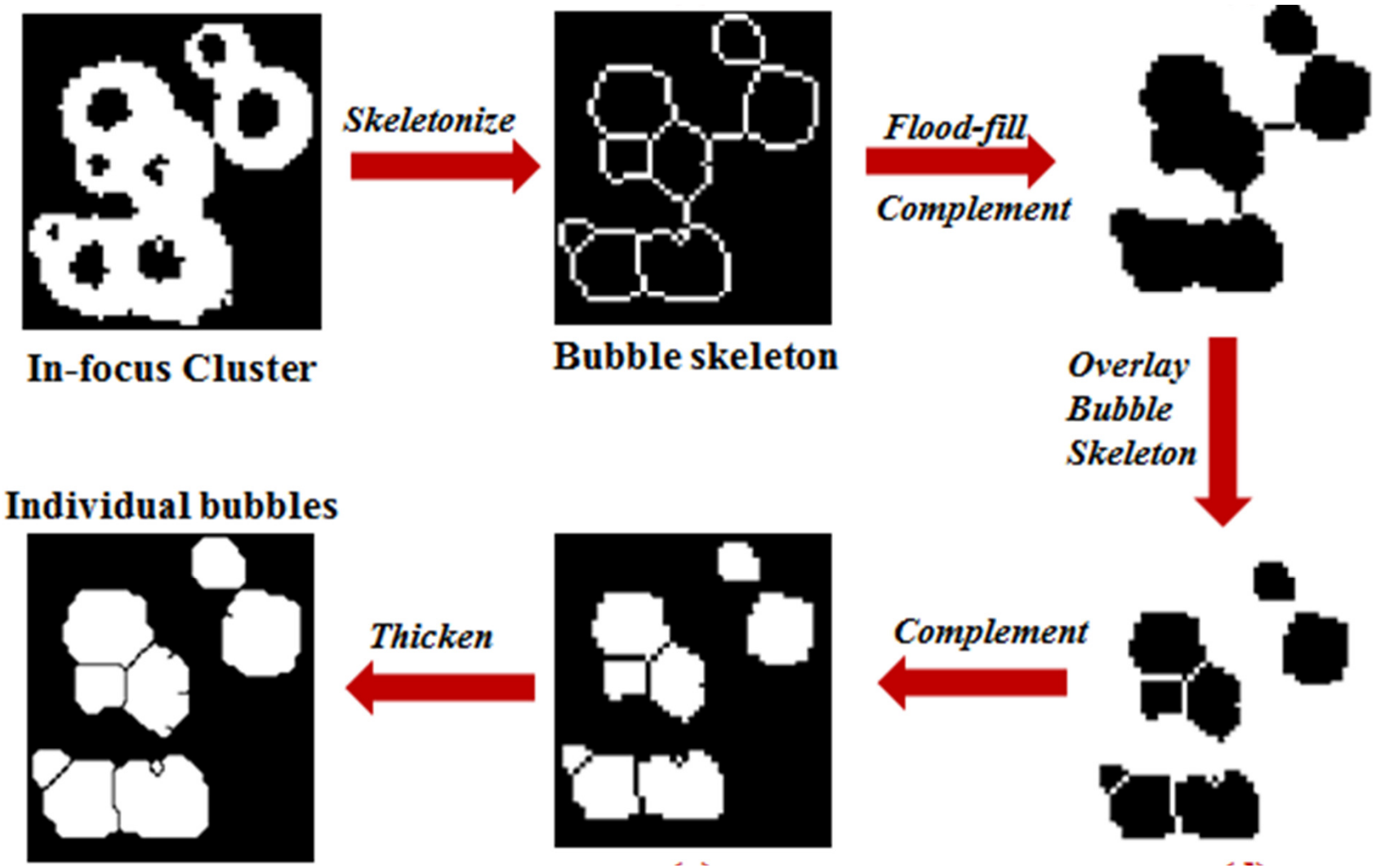

Bubble size and shape measurements

- Labelled bubble regions are first grouped into : Small, Intermediate and large bubbles based on an area threshold.
  - Small bubbles are necessarily assumed to be spherical. (Area, A <10 pixels)
  - Large bubbles are necessarily passed through a cluster-processing step.
  - Intermediate or large individual bubbles can be either spherical or ellipsoidal.
- Shape is determined by *Heywood Circularity Factor* (*HCF*).

$$HCF = P/\sqrt{4\pi A} \text{ (= 1 for a spherical bubble)}$$

$A < 10$ pixels | $0.9 <$ HCF < 1.15	$HCF < 0.9 \mid HCF > 1.15$
$d = \sqrt{4A/\pi}$	*Use ellipsoidal fitting*

Technique Validation

- **Simulation of synthetic bubble images**
  - Single Bubble Measurement
  - Polydisperse Bubble Size Distribution Measurement

- **Experimental Validation**

Validation through Simulation

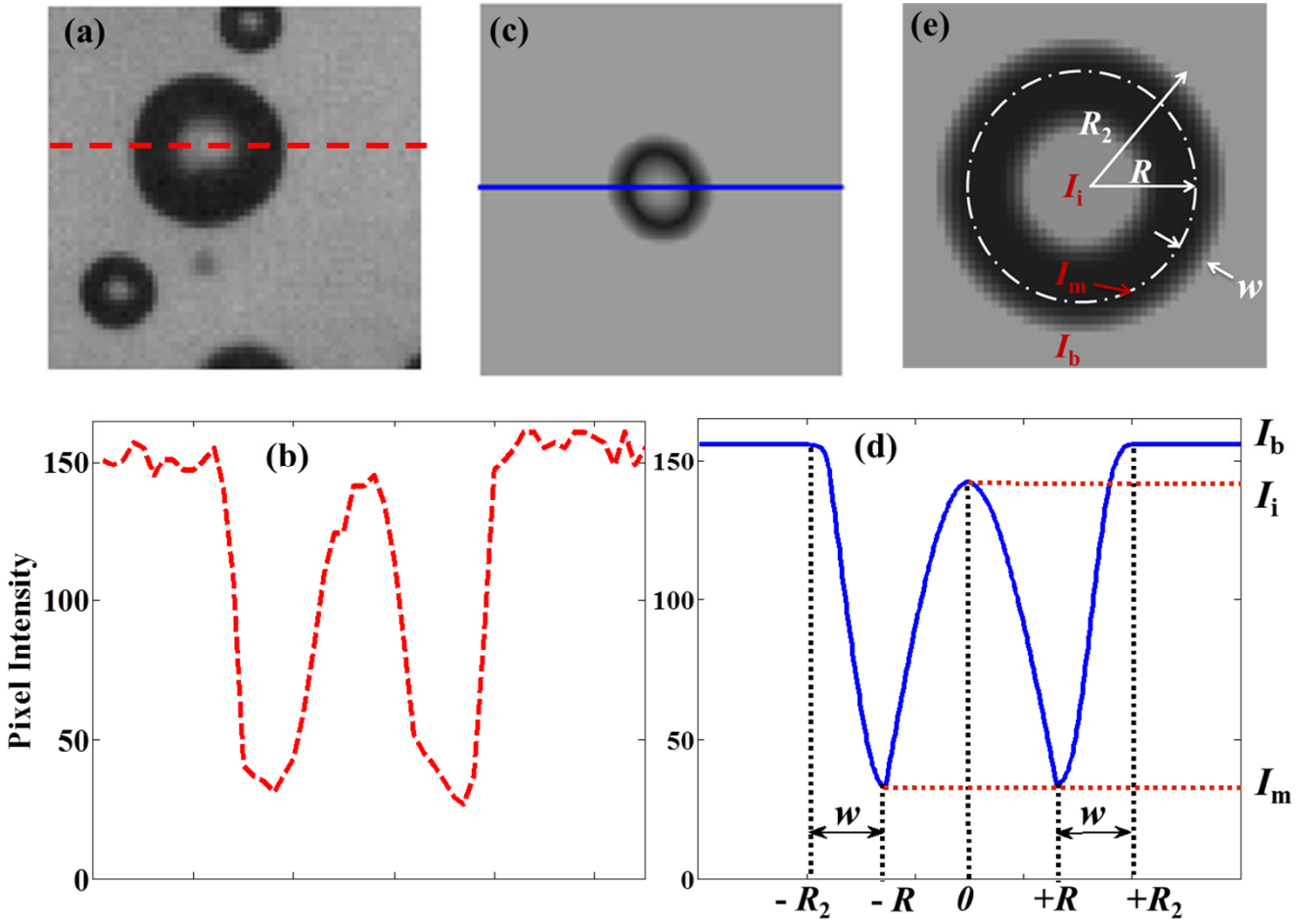

Synthetic Bubble Generation Procedure

$$I = ar^2 + b$$

$$a = \frac{(I_m - I_i)}{R^2}\,;\, b = I_i \qquad if\ |r| < R$$

$$a = \frac{(I_b - I_m)}{(R_2^2 - R^2)}\,;\, b = I_m - \frac{(I_b - I_m)R^2}{(R_2^2 - R^2)} \qquad if\ R_2 > |r| > R$$

Single Bubble Measurement

- A bubble is drawn with a specific radius with its centroid placed in the middle of a pixel.
- 50 similar new bubbles are generated with centroid translated with steps of 0.01 pixels.

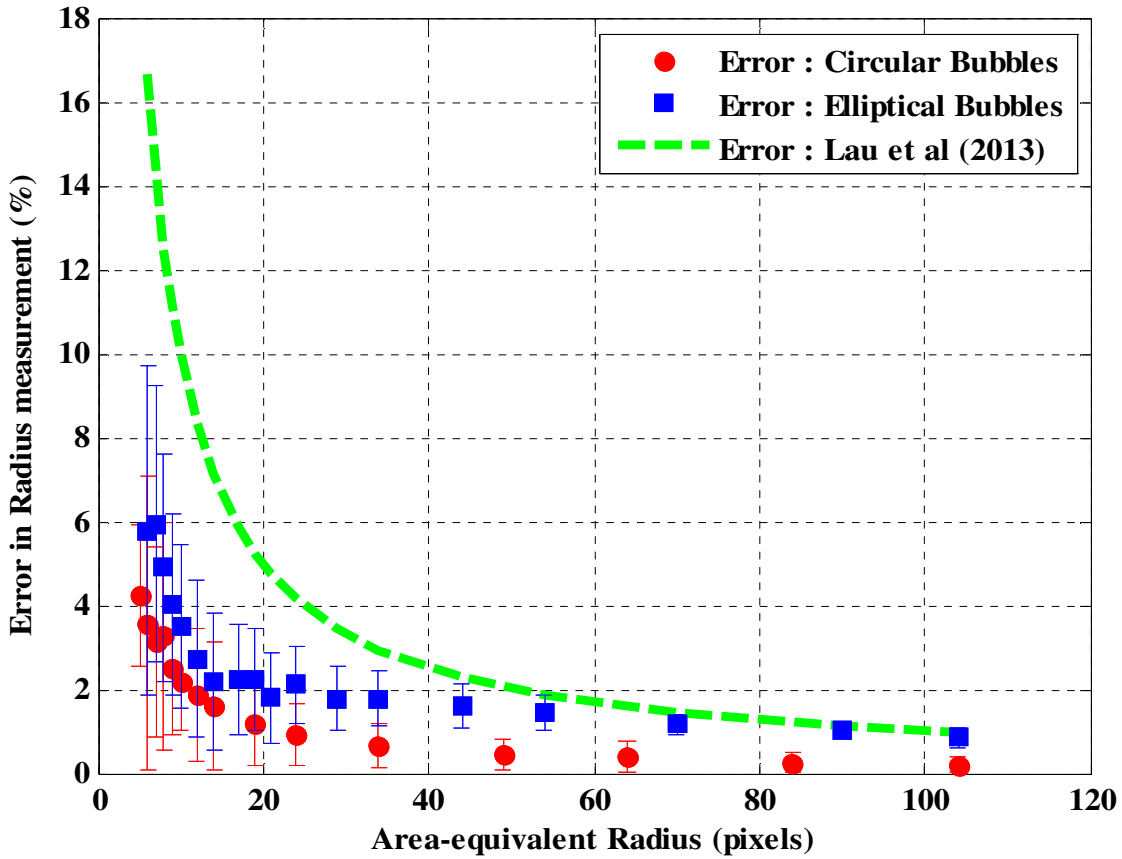

Polydisperse Bubble Size Distribution Measurement

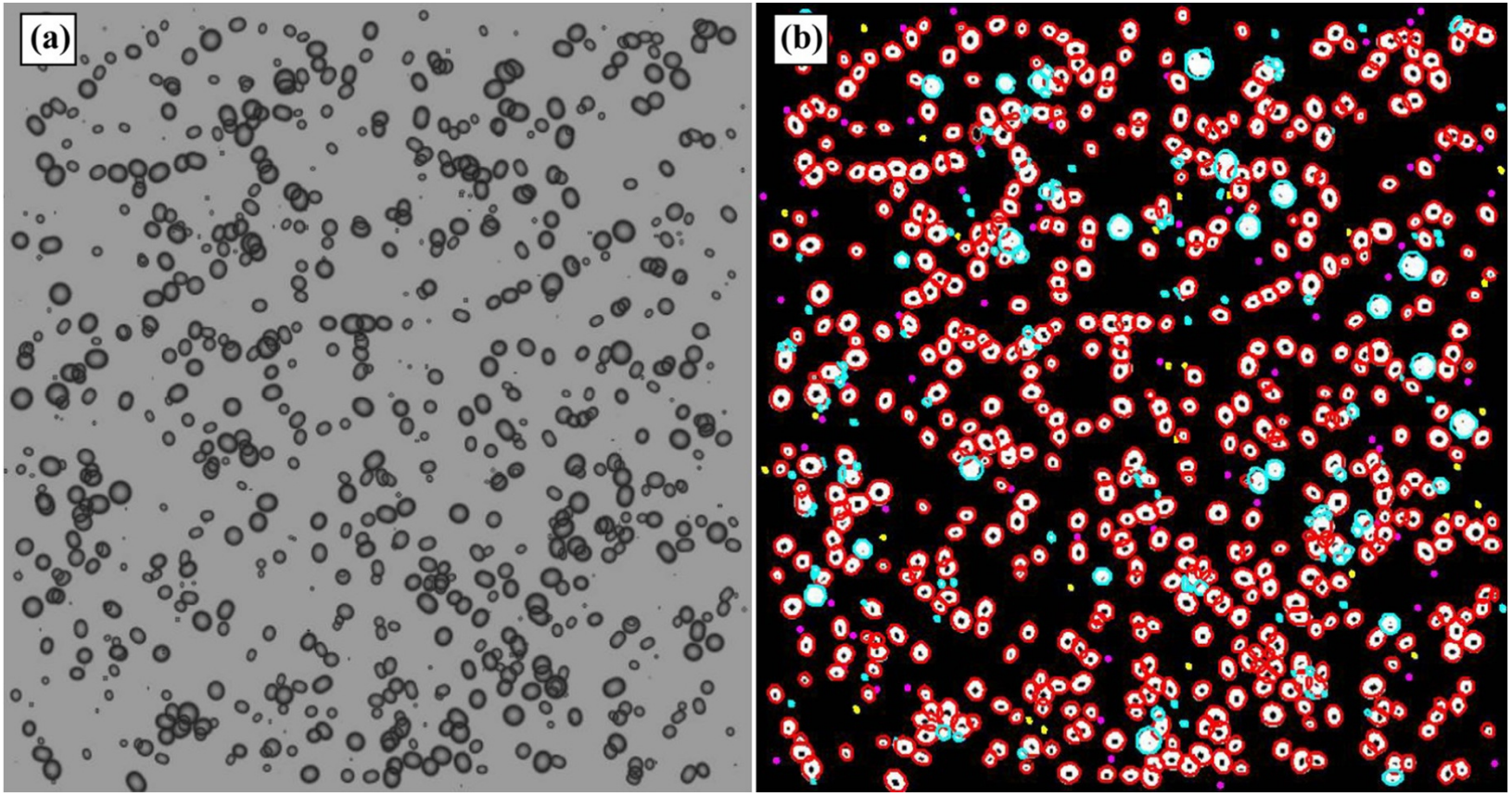

- Bubble images were generated with void fraction ranging from 0.1 - 0.7, with bubble eccentricity randomly chosen between 0 – 0.9.
- Figure above shows a bubble image with 900 bubbles.

Polydisperse Bubble Size Distribution Measurement

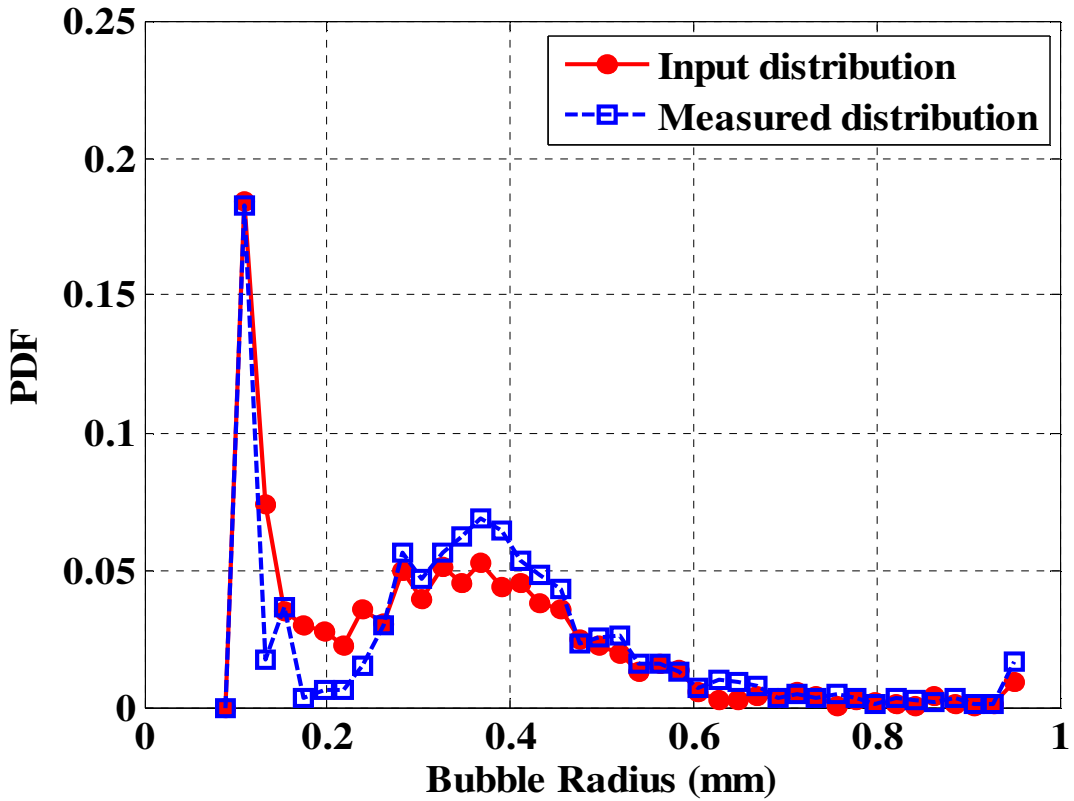

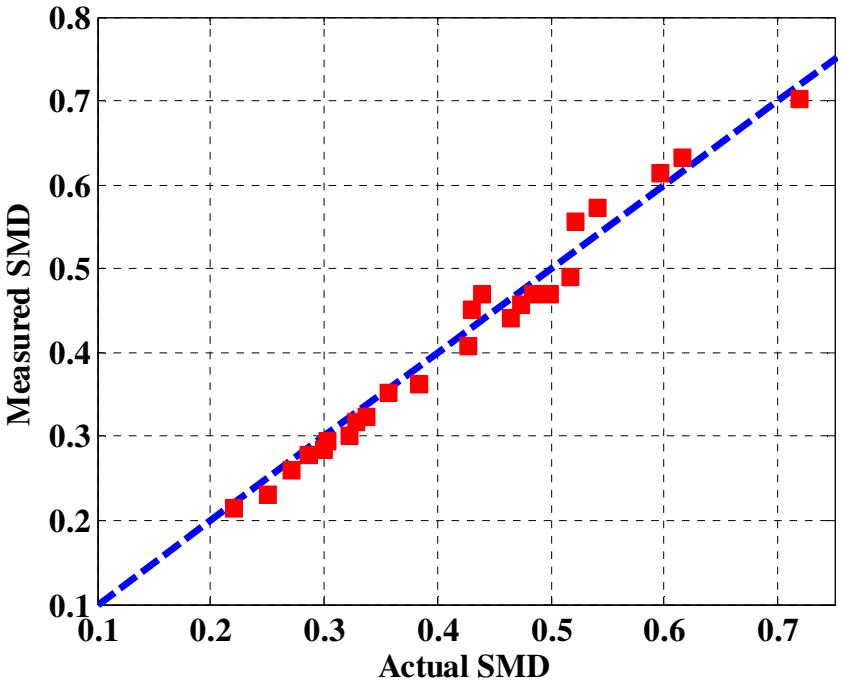

- The image-processing algorithm captures the bimodal distribution quite well and the magnitudes in the PDFs are in good agreement.

- The measured SMD is in good agreement with the input results with errors staying within 6-8% (limitation in accurately resolving highly overlapping bubble clusters).

Experimental Validation

- Extract 2D bubble size information,
- Obtain the volume and velocity of individual bubbles, and
- Calculate the volume flow rate from the volume and velocity information

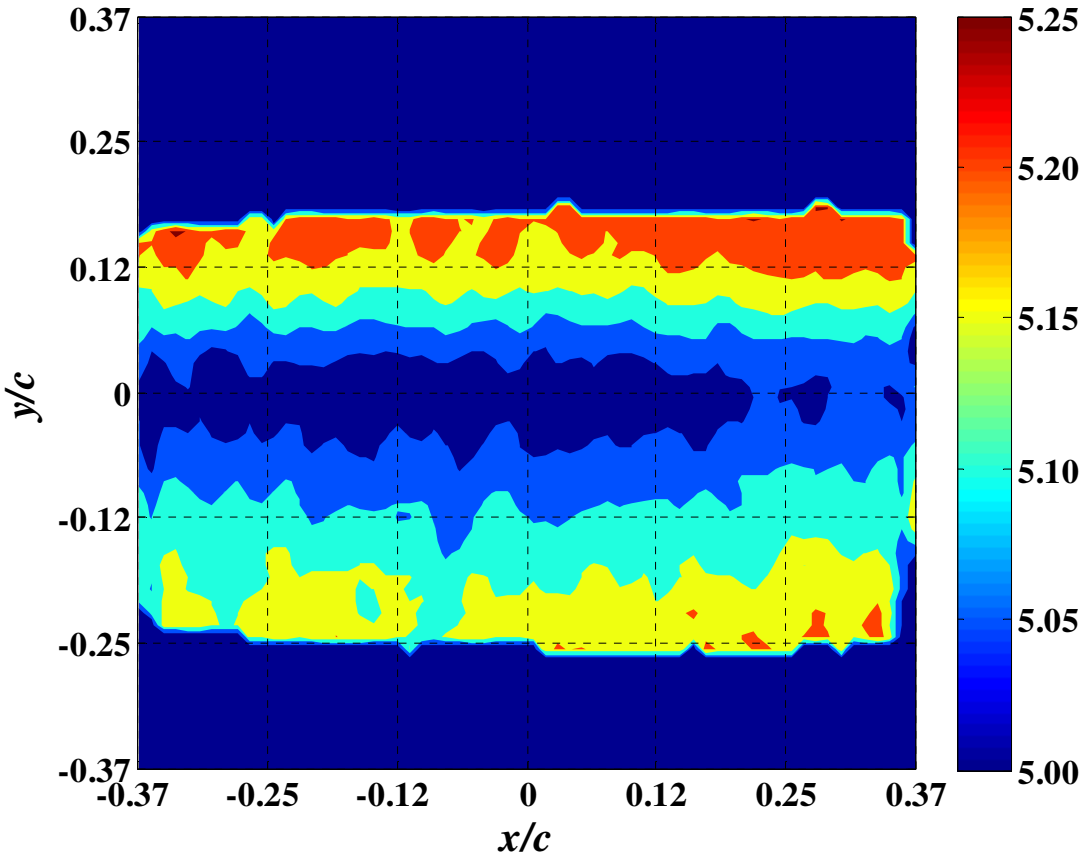

Bubble Velocity Field

Experimental Validation

$$\dot{Q}_{single} = \sum_{i=1}^{N} \left(\frac{u_i}{w}\right)\left(v_i \times \frac{P_{TS}}{P_0} \times \frac{T_0}{T_{TS}}\right); \qquad v_i = (4\pi/3)a_i b_i^2$$

Volume flow rates thus obtained are averaged over 1000 images to estimate an averaged volume flow rate.

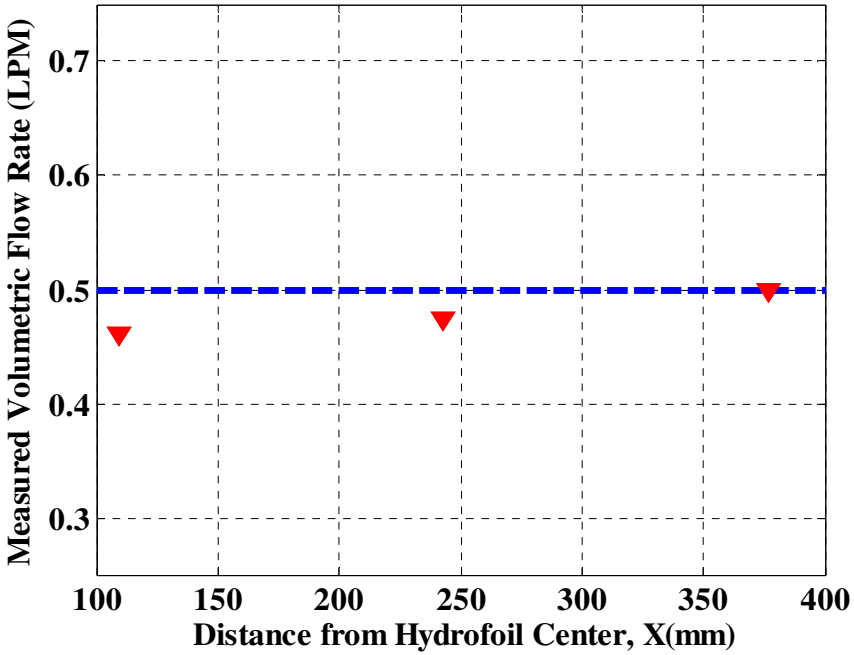

Bubble Size Characterization

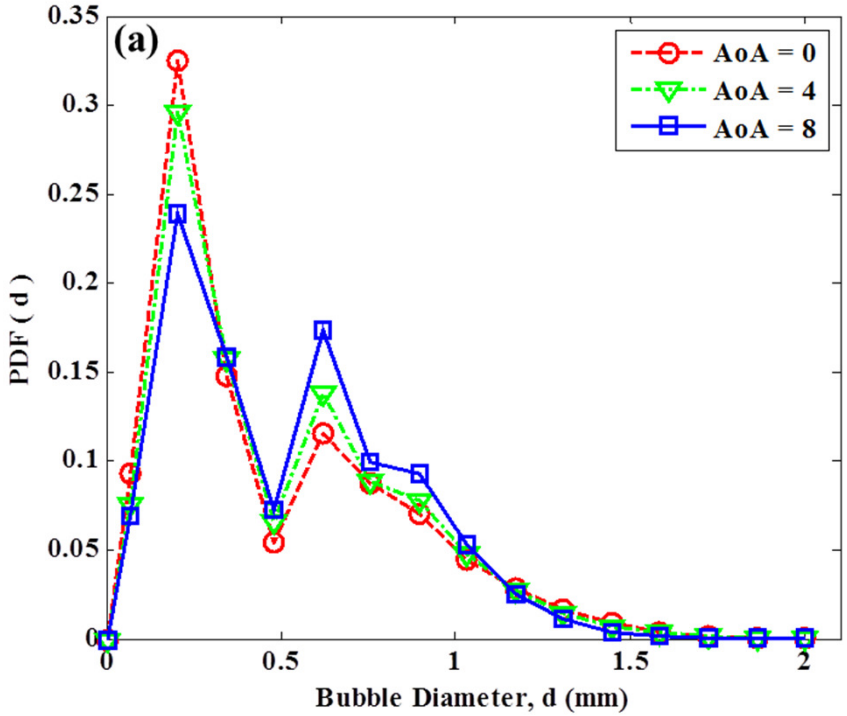

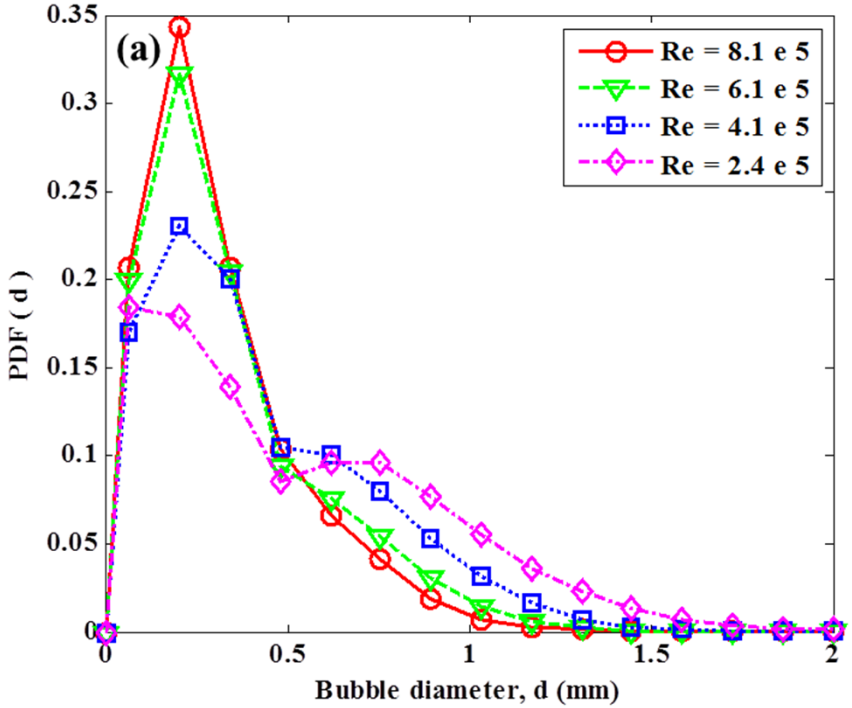

- A bimodal bubble size distribution is obtained with two modes at 0.2 and 0.6 mm.
- An excess of **tiny** bubbles (~0.2 mm) are observed.
- Some extremely large size bubbles (>2 mm) are observed **even far downstream**.

Karn et al., Exp. Therm. Fluid Sci. 2015b

The effect of increased ventilation

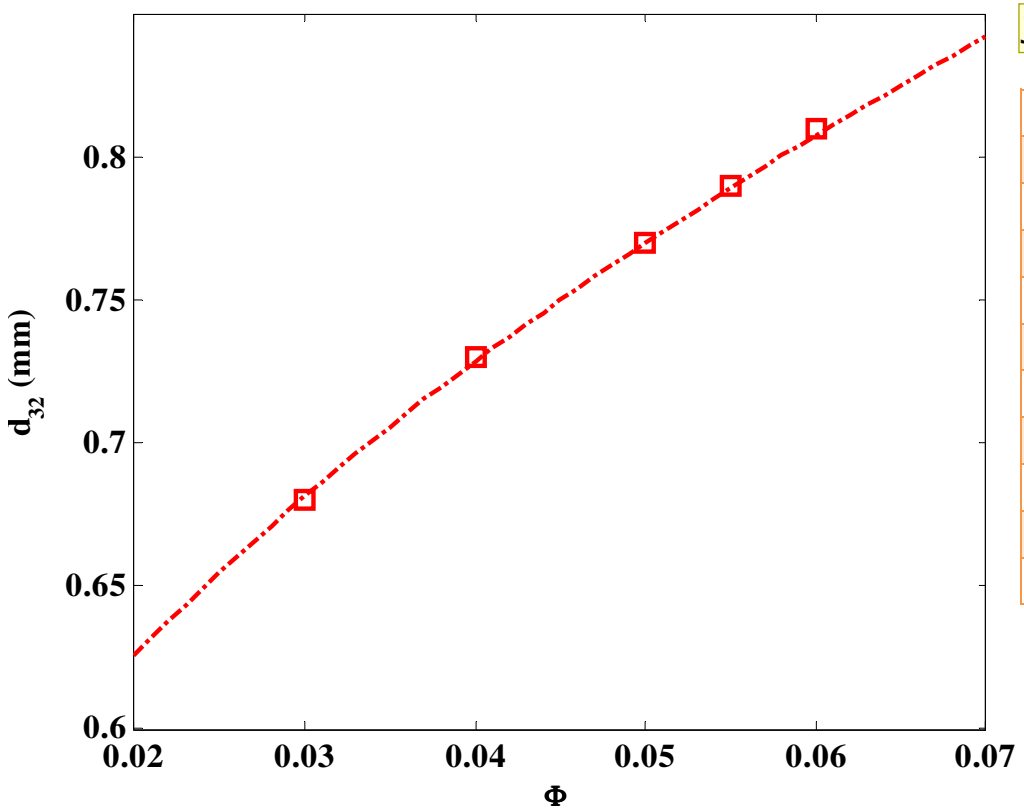

JH30

V (m/s)	Q (LPM)	ϕ	N/(1e6)	$D_{99.8}$	SMD
10	1.50	0.091	2.382	0.95	0.54
10	0.50	0.047	1.805	0.78	0.43
7.5	1.13	0.059	1.325	1.03	0.60
7.5	0.50	0.036	1.068	0.89	0.51
5	1.50	0.065	0.782	1.38	0.81
5	1.25	0.057	0.723	1.35	0.79
5	1.00	0.050	0.677	1.31	0.77
5	0.75	0.042	0.645	1.24	0.73
5	0.50	0.032	0.573	1.16	0.68
3	0.50	0.028	0.242	1.62	0.97

- The increase in ventilation (or the void fraction) leads to greater d_{32} and greater number of large sized bubbles.
- This happens because of increased coalescence events in the wake.

Slide 24

JH30 This slide should be removed.
Jiarong Hong, 20-11-2014

Insight into Bubble Coalescence/ Splitting

Total Number of Bubbles (NOB) passing through each section

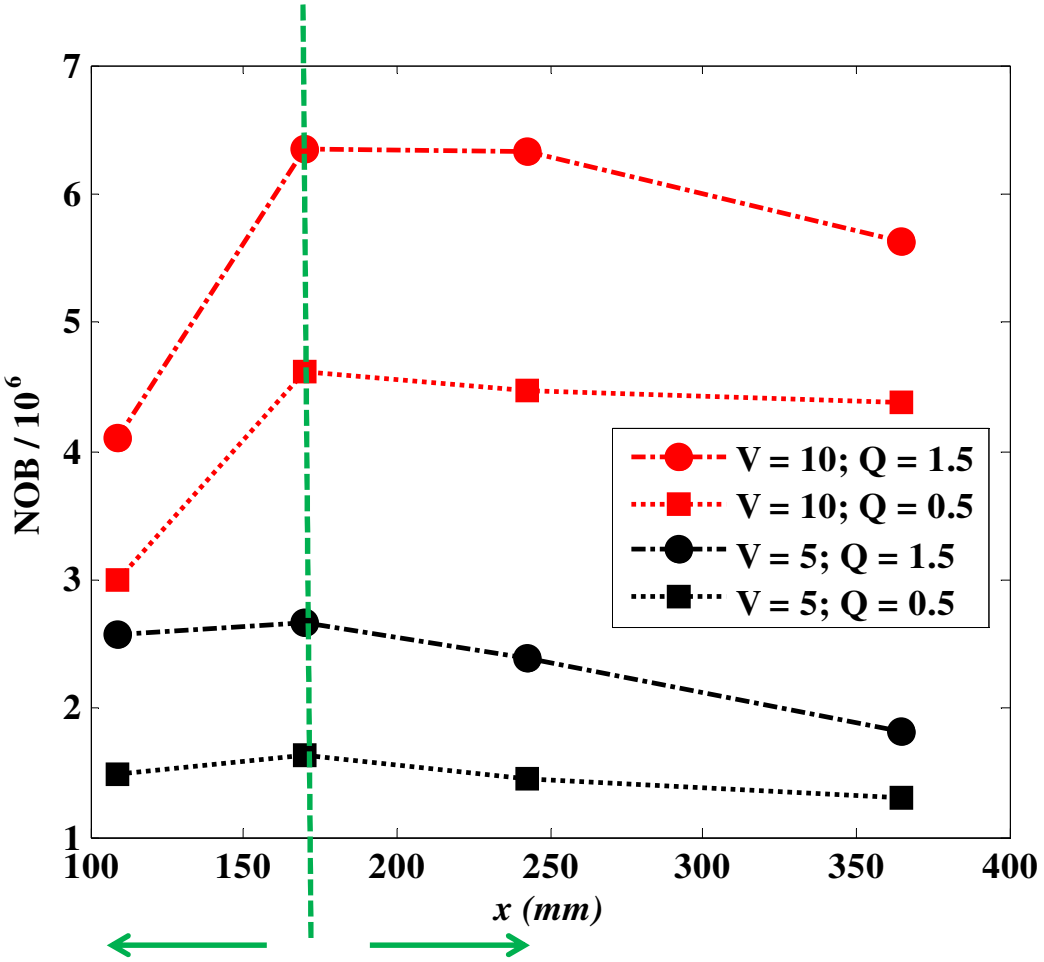

x = 0 – 170 mm :
Break-up dominant regime

x > 170 mm :
Coalescence-dominant regime

Bubble size distribution in the breakup-dominant regime

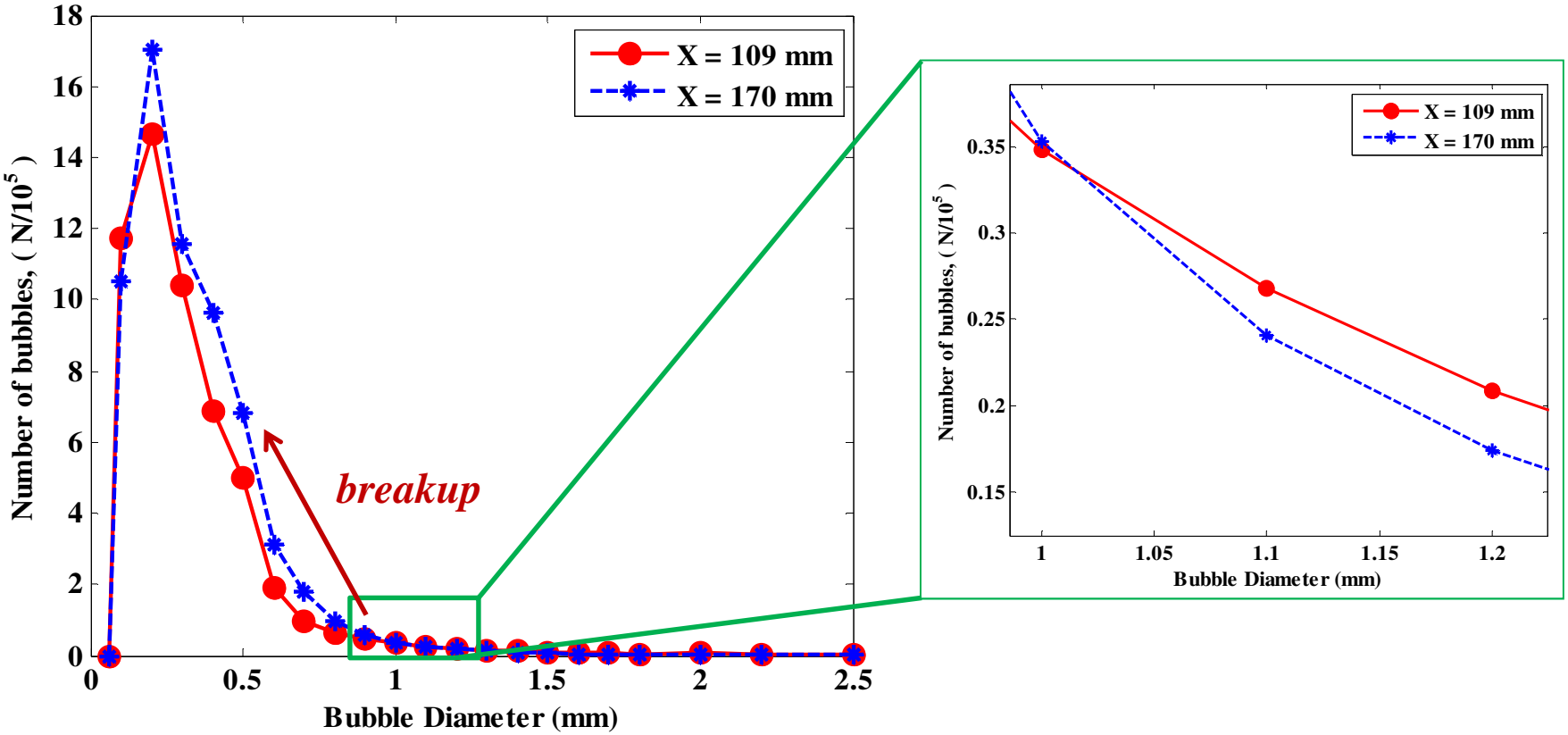

- Larger bubbles breakup to give smaller bubbles in the region between X = 109 mm and X = 243 mm.

Bubble size distribution in the coalescence-dominant regime

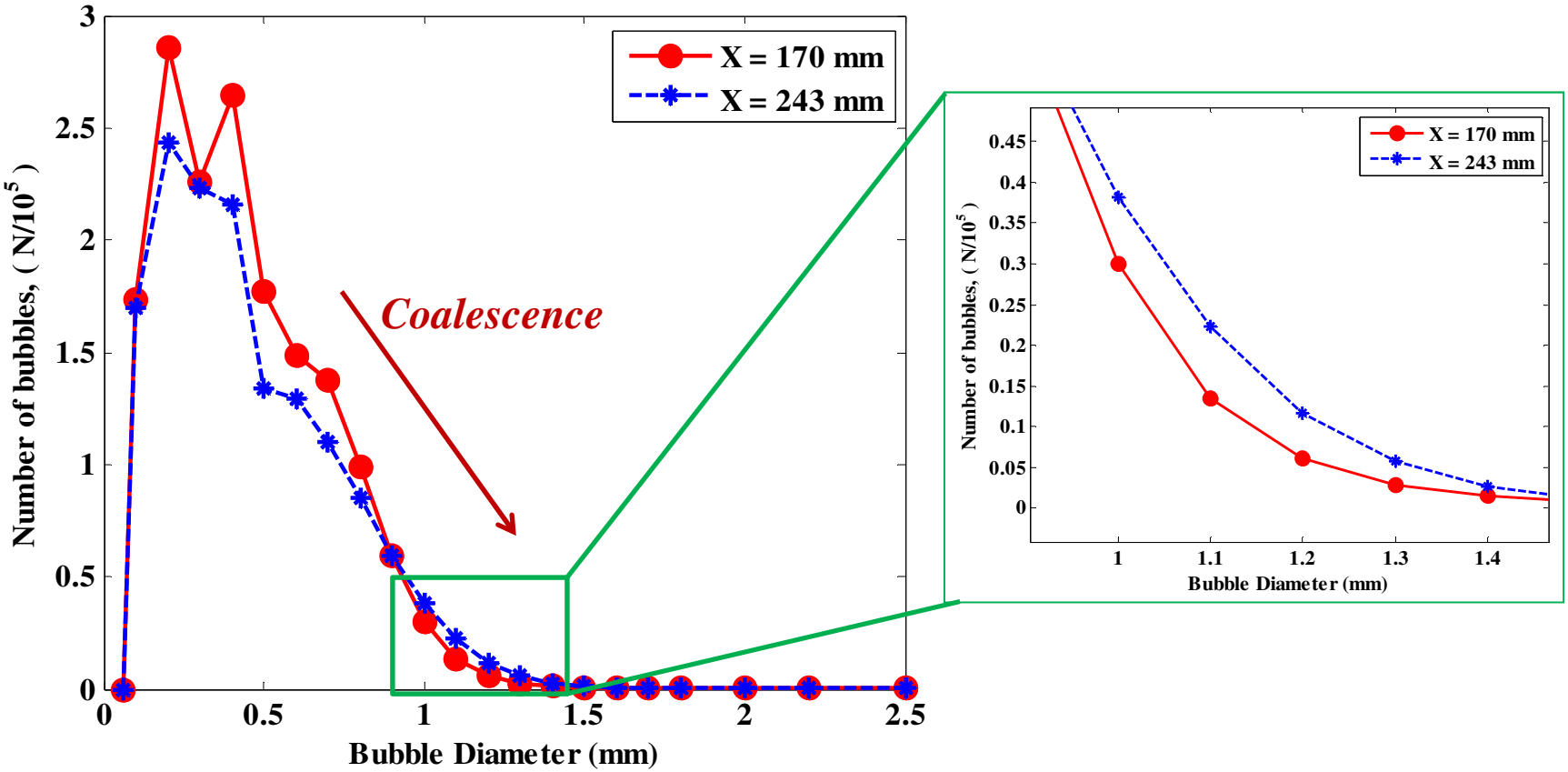

- Smaller bubbles coalesce to give larger bubbles in the region between X = 170 mm and X = 243 mm.

Observations on Bubble Breakup

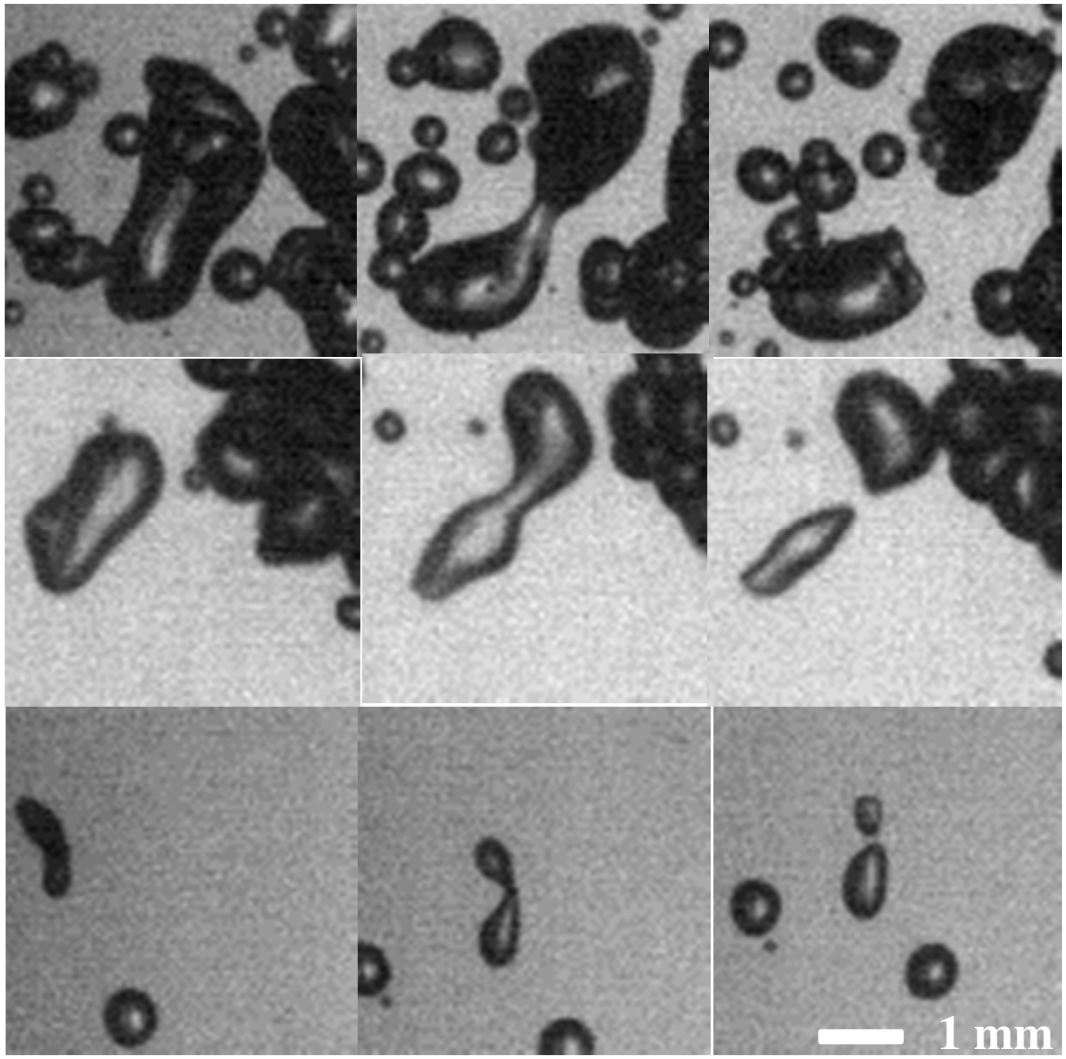

- The observed bubble breakup events are always binary.
- No generation of small bubbles (0.2mm) during binary break up
- The initial bubble sizes are always greater than 1.5 mm in all cases.

Where do these small bubbles come from ?

JH11

Slide 28

JH11 The font is not consistent

change the font size of all the bullet point to 20
Jiarong Hong, 20-11-2014

Mechanism I: Bubble Tearing

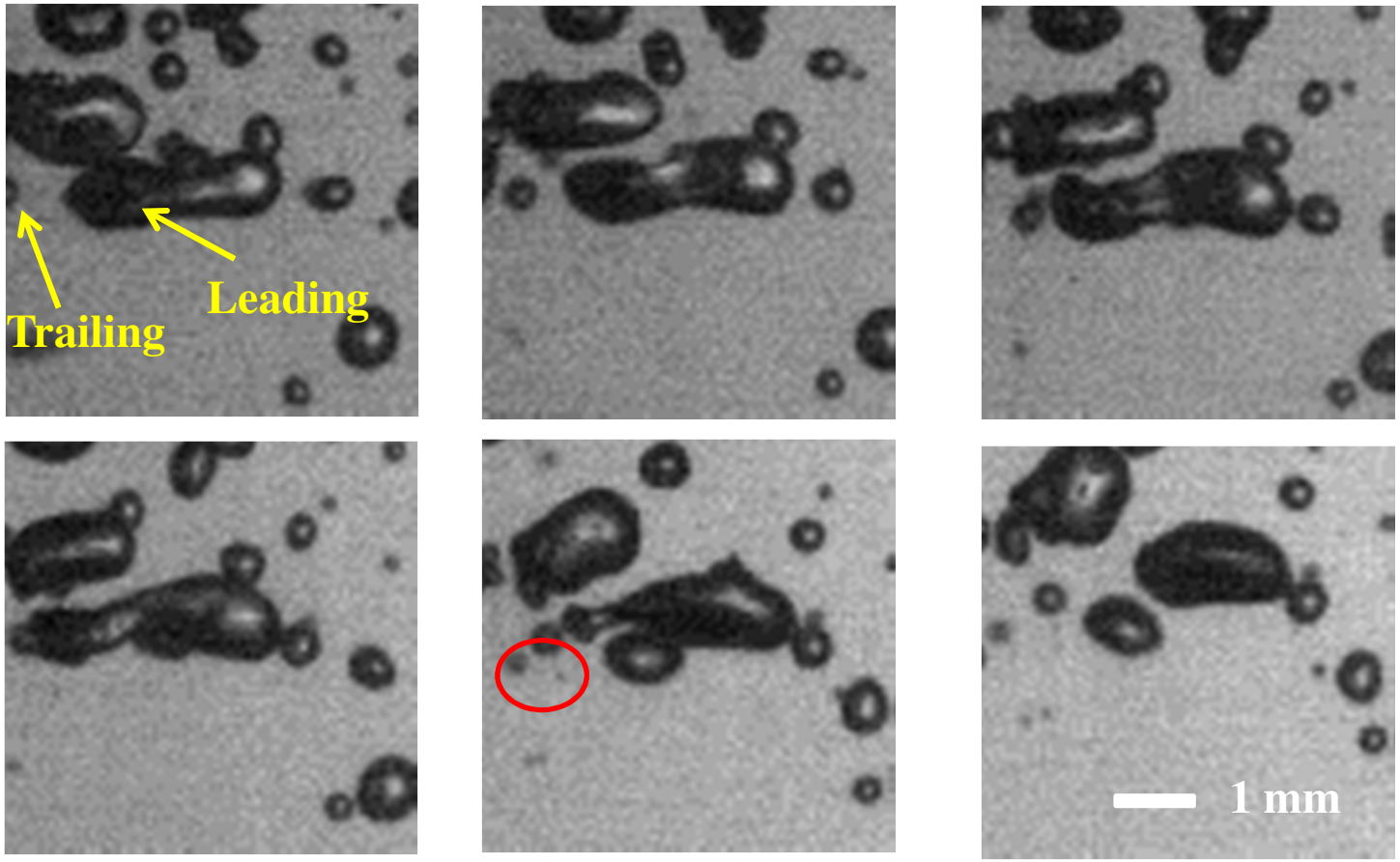

- Wake acceleration of a trailing bubble and collision with a leading bubble leads to bubble tearing and small bubble generation.

JH13

Slide 29

JH13 remove
Jiarong Hong, 20-11-2014

Mechanism II: Bubble generation during Coalescence.

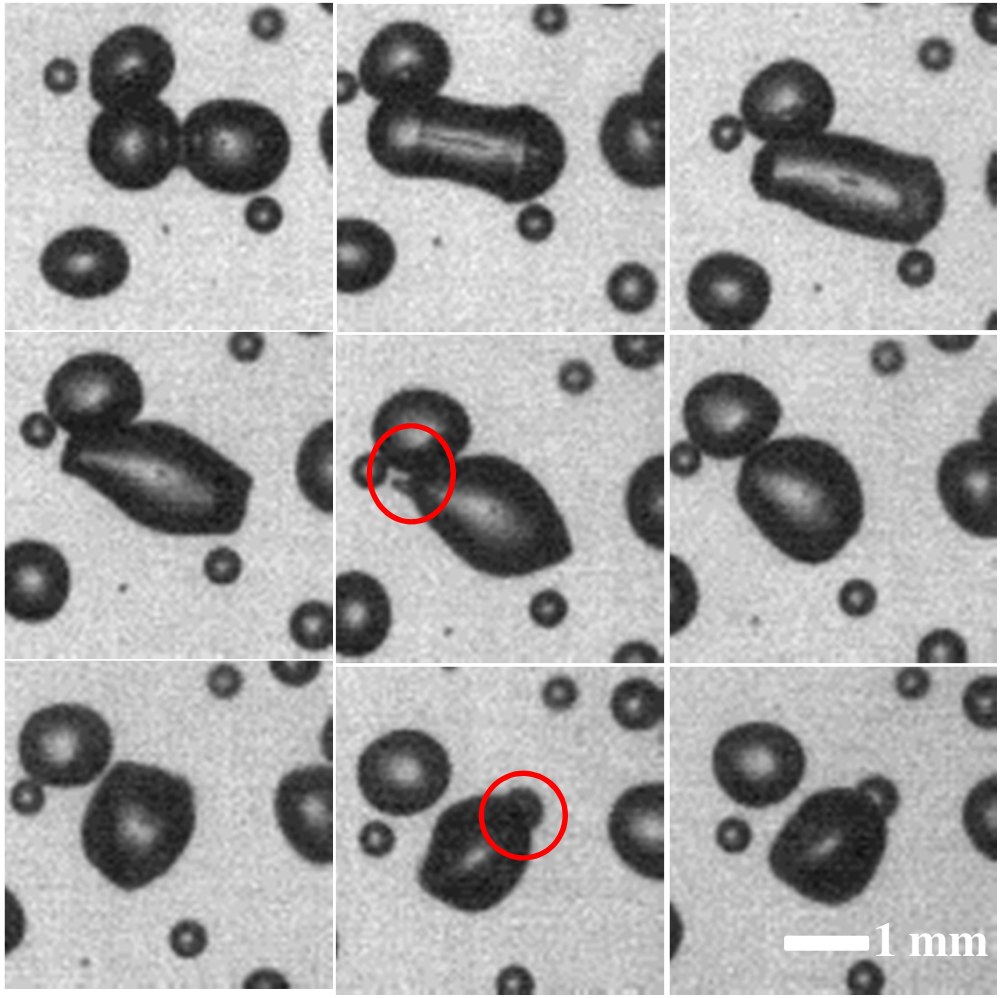

- Careful observation of coalescence events shows that after a coalescence event, the bubbles undergo severe shape oscillations, and sometimes form tiny bubbles.

Coalescence-mediated Breakup

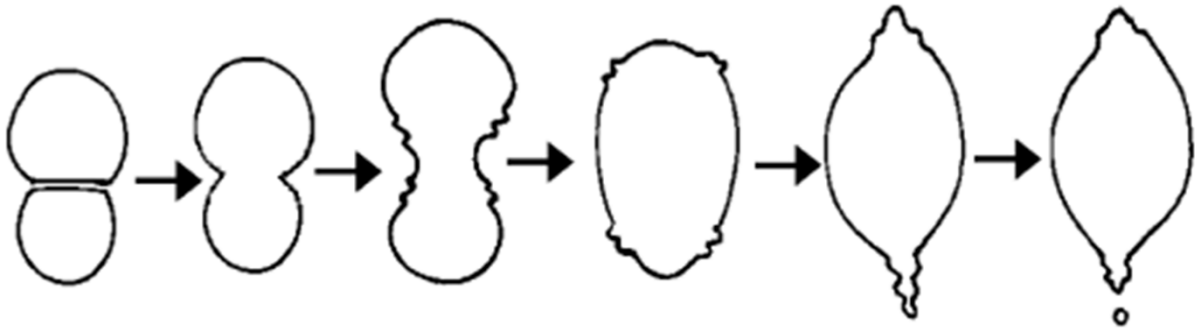

Tse et al. (2000)

- An ellipsoidal bubble forms two lobes at the end which may be separated by Rayleigh instability (*Ohnishi 1981*).

- After the lobe separation, the ellipsoidal bubble contracts and transitions into a spherical cap bubble before returning to a spherical bubble.

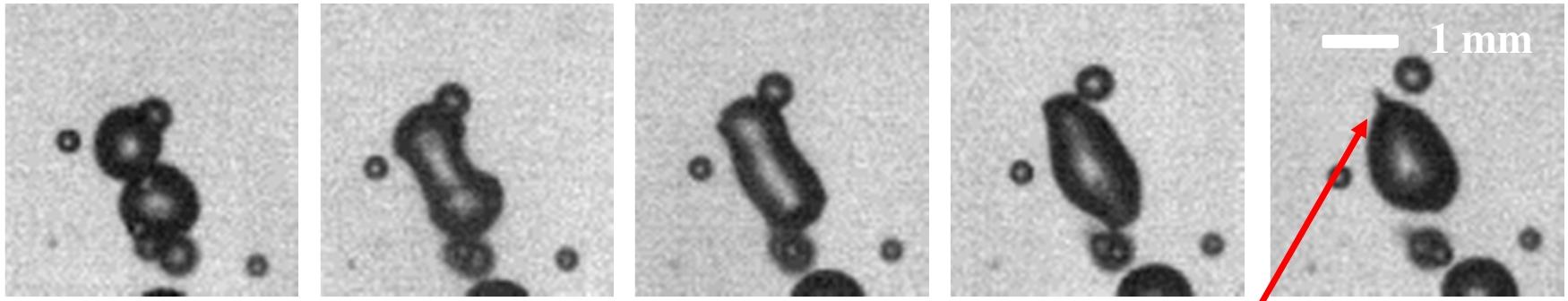

Slide 31

JH29 font too small!
Jiarong Hong, 20-11-2014

Large Bubble Generation I: Successive Coalescence Events

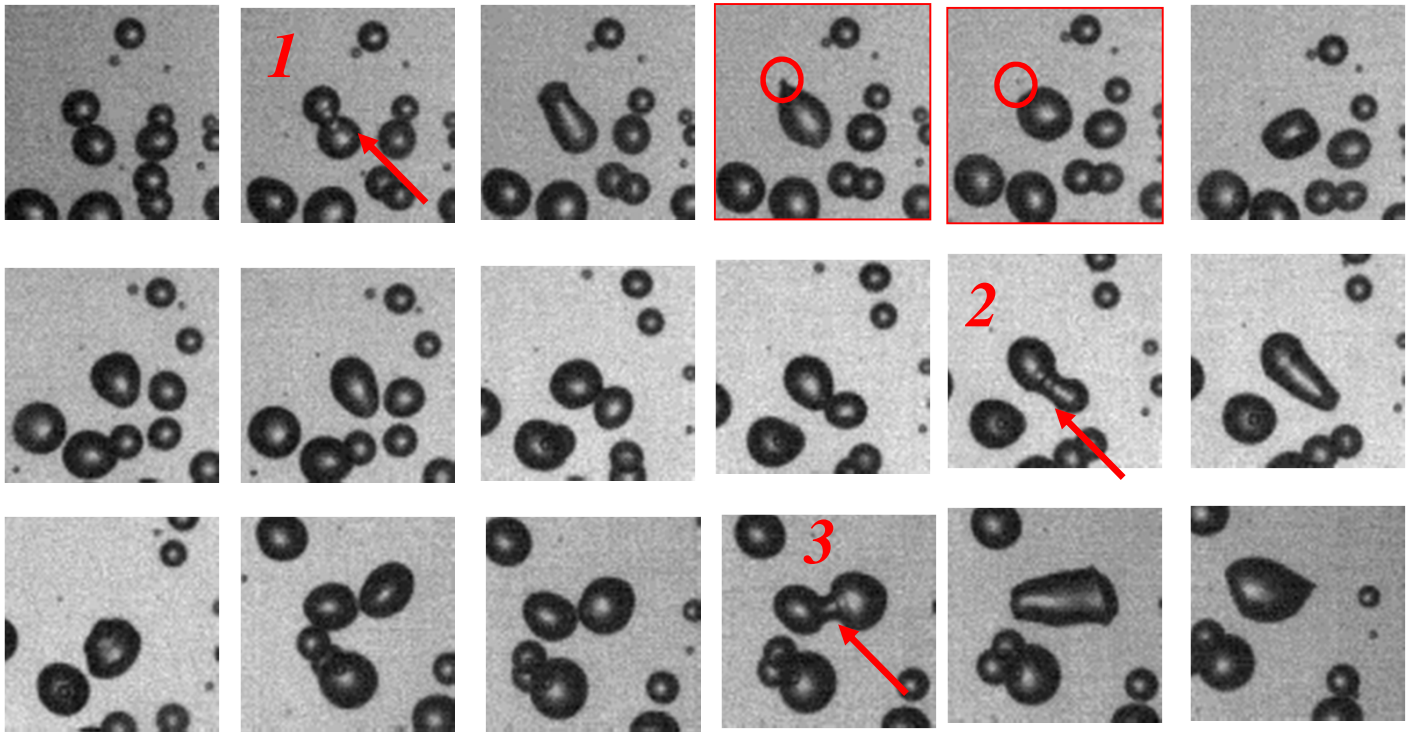

- In general, successive coalescence events lead to larger size bubbles.
- However, within a small of observation, successive binary coalescence events will not lead to bubbles with sizes greater than 3 mm.

Large Bubble Generation II: Cluster Coalescence

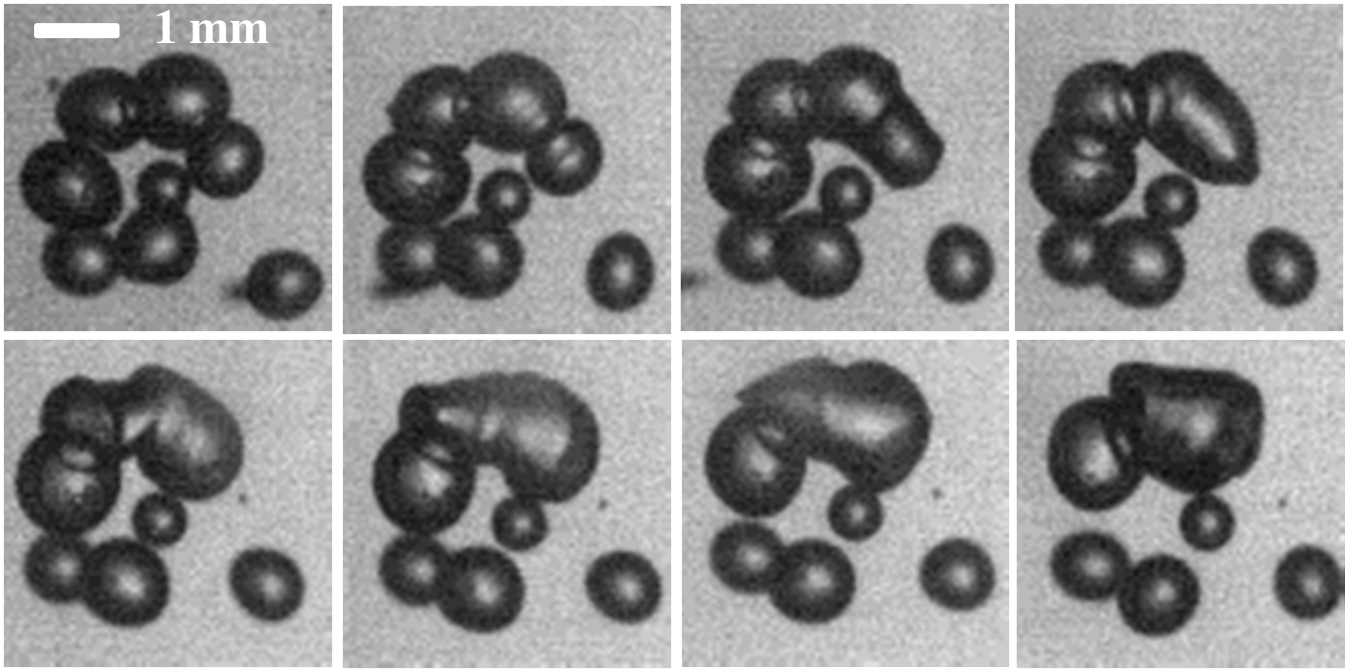

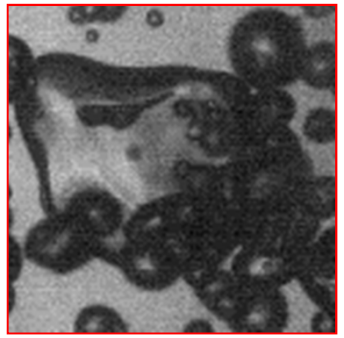

- Usually, the coalescence events are binary. However, sometimes exceptions involving multiple bubbles are also possible.

- The presence of extremely large bubbles far down in the wake can be explained by the phenomenon of ‘cluster coalescence’.

Conclusions

- A robust image analysis technique was developed to extract bubble size and shape information in a dense bubbly flow over a wide size range.
- The developed technique was validated through both bubble simulation and experimental measurements.
- The image analysis technique showed the occurrence of distinct breakup and coalescence regimes in the wake.
- The occurrence of breakup and coalescence was actually confirmed by high-speed observations.

Acknowledgements

This project is supported by grants from

DOE EERE Wind & Water Power Program

Dr. Jose Zayas, Program Manager

ONR, Dr. Ron Joslin, Program Manager.

Alstom Énergie & Transport Canada Inc.

Mr. Michel Sabourin, Program Manager


Thank you !
TOP FLITE
1
Questions or Comments?
http://umn.edu/~karn